Semicond. Sci. Technol. **14** (1999) 419–424. Printed in the UK PII: S0268-1242(99)98599-1

Study of temperature effects on loss mechanisms in 1.55 μm laser diodes with $In_{0.81}Ga_{0.19}P$ electron stopper layer

P Abraham†, J Piprek, S P Denbaars and J E Bowers

Department of Electrical and Computer Engineering, University of California Santa Barbara, CA 93106, USA

Received 21 October 1998, accepted for publication 2 February 1999

Abstract. The importance of the electron loss from the separate confinement layer (SCL) to the p-cladding in 1.5 μm lasers is analysed comparing two structures. One is a regular structure with strained InGaAsP quantum wells and a 1.15 μm emitting InGaAsP SCL and the second one incorporates an additional $In_{0.81}Ga_{0.19}P$ electron stopper layer (about 50 meV high) at the interface between the p-cladding and the SCL. The results are analysed using comprehensive simulation software. It is shown that the current leakage at the SCL p-cladding interface is not the dominant loss phenomenon at room temperature. Instead, the inhomogeneity of the carrier injection over the QWs is identified as being mainly responsible for the non-unit internal quantum efficiency. The inhomogeneity increases above threshold with the current injection and produces increasing carrier recombination losses. However, at higher temperature (above 60 °C) the additional $In_{0.81}Ga_{0.19}P$ electron stopper layer is efficient to decrease the electron leakage from the SCL to the p-cladding. It is also shown that besides the beneficial effect of improving the internal quantum efficiency at high temperature the electron stopper layer also slightly increases the threshold current by increasing the carrier density and the absorption loss in the SCL. Finally, our measurements show that above a critical temperature (97 °C in this case) the SCL absorption loss increases dramatically.

1. Introduction

The phenomena leading to carrier and stimulated photon losses in lasers are rather well known. For carrier losses it is Shockley–Read–Hall recombination, spontaneous emission, Auger recombination and electron leakage through spreading current or escape from the active region into the p-cladding region. For long-wavelength lasers there is strong evidence that the temperature sensitivity of the threshold current is mainly controlled by Auger recombination [1]. However, it is not as clear for the temperature sensitivity of the differential quantum efficiency (slope efficiency). The differential quantum efficiency is controlled by the internal quantum efficiency, by internal absorption and by the mirror reflectivity.

The non-unit value of the internal quantum efficiency is the result of the carrier loss increase above threshold. In the case of an ideal laser with the carrier density clamped to its threshold value the internal quantum efficiency should be 1. Even at room temperature this is not the case in actual lasers and to understand and improve the temperature behaviour of long-wavelength lasers it is important to know what loss mechanism is mainly responsible for the non-unit value of the internal quantum efficiency.

For 1.3 μm lasers, loss outside the active region is important because the conduction band offset between the InP cladding layer and the separate confinement layer (SCL) is small [2]. Although this is not as critical for 1.55 μm lasers it still has to be taken into account. Belenky and co-workers pointed out the importance of the leakage current from the SCL for 1.3 μm lasers [3]. In particular, they investigated experimentally and theoretically the effect of the p-doping profile of the cladding layer of a 1.3 μm emitting laser. In the case of an undoped p-cladding–SCL interface they show that at 323 K (50 °C) the electron leakage current reaches 20% of the total injection current at an injection current density of 10 kA cm^{-2}. Different solutions were proposed to reduce this phenomenon. One is to introduce p-doping at the p-cladding–SCL interface or even in the SCL. This is indeed an efficient way to increase the energy difference between p-cladding and active region conduction bands. However, it also increases the optical loss due to free carrier absorption and inter-valence band absorption (IVBA) in the SCL where the confinement factor is important. Another solution proposed for 1.3 μm lasers is to grow the structure in the InGaAlAs/InP system. It is then possible to take advantage of the type II interface

† On leave from Laboratoire Multi-Matériaux et Interfaces, Université C Bernard Lyon 1, France. E-mail address: abraham@opto.ucsb.edu

 © 1999 IOP Publishing Ltd

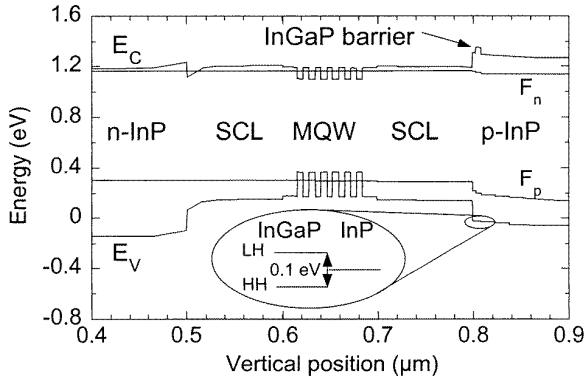

Figure 1. Energy band diagram of laser structure with $In_{0.81}Ga_{0.19}P$ electron barrier near threshold at room temperature. The insert shows the light-hole (LH)–heavy-hole (HH) split-up of the $In_{0.81}Ga_{0.19}P$ valence band. E_C and E_V are the conduction and valence bands and F_n and F_p are the electron and hole quasi-Fermi levels.

between InP and $In_{0.52}Al_{0.48}As$ to introduce an electron barrier layer on the p-side using $In_{0.52}Al_{0.48}As$ and a hole barrier layer on the n-side using InP [4]. However, in that case the difficulty is in the growth of Al containing alloys. The typical oxygen concentration in MOCVD grown $In_{0.52}Al_{0.48}As$ is in the 10^{17}–10^{18} cm^{-3} range [5]. It produces deep n-type levels that increase the internal absorption loss and the threshold current density. For 1.55 μm lasers the internal absorption loss and the threshold current density have been reported to be respectively as high as 27 cm^{-1} and 1.1 kA cm^{-2} for 6 QW GaInAlAs lasers (400 μm cavity length) [6]. In the InGaAsP system for the same number of wells and the same cavity length these values are of the order of 10 cm^{-1} and 0.6 kA cm^{-2} in our work. An intermediate approach, utilizing InGaAsP QW and InGaAlAs barriers with an $In_{0.52}Al_{0.48}As$ electron stopper layer has also been investigated [7]. In that case the internal absorption losses are again in the 20 cm^{-1} range, but the electron stopper layer was demonstrated to be efficient to decrease the leakage current. The use of electron stopper barriers between the SCL and the QW has also been investigated. This was also demonstrated to be efficient but it is necessary to introduce p-doping in the electron stopper barrier to avoid any additional barrier for holes in the valence band [8, 9]. Again, the p-doping increases the absorption loss and the threshold current. For that type of structure to have no drawbacks it would be necessary to use a material with a valence band energy in between that of the SCL material and that of the QW barrier.

It was also proposed to use multi-quantum barriers to create a virtual barrier on the p-side of the SCL. The advantage in that case is that the energy of the barrier introduced can be large and that it does not require the use of Al or p-doping of the SCL [10]. However, it is also essential that the design of the barrier does not hinder hole injection in the active region.

To obtain more insight into the phenomena reducing the internal quantum efficiency at room temperature and higher temperatures we report in this paper on a simple modification of the classical InGaAsP laser structure increasing the electron confinement in the SCL. It consists of increasing the conduction band offset between the cladding layer and the SCL on the p-side. For that purpose, a thin $In_{0.81}Ga_{0.19}P$ layer is inserted between the p-InP cladding layer and the SCL. The conduction band energy of $In_{0.81}Ga_{0.19}P$ is higher than that of InP and introduces a barrier in the conduction band. This barrier is about 50 meV at 4 K [11] and can be estimated to be close to that value at room temperature using the model-solid theory [12]. The light-hole band gap energy of $In_{0.81}Ga_{0.19}P$ coherently strained to InP is almost the same as that of InP and the splitting between the light-hole and heavy-hole valence bands is about 100 meV. Figure 1 shows the band diagram of the active region with the $In_{0.81}Ga_{0.19}P$ barrier and a detailed sketch of the valence band lineup at the $In_{0.81}Ga_{0.19}P/InP$ interface. It can be seen that the injection of holes through the light-hole valence band of $In_{0.81}Ga_{0.19}P$ can be achieved without overcoming a barrier. So, no p-doping is necessary in this layer to avoid any barrier for hole injection in the active region.

Section 2 describes the structures with and without additional electron barrier layer (thereafter called respectively structures W and W/O). Section 3 describes how the absorption loss and internal quantum efficiency are measured and compares the experimental results achieved with structures W and W/O. These results are analysed in section 4 by simulation of both structures using advanced laser software [13].

2. Device structures

The laser structures were grown in a metal–organic vapour phase epitaxy horizontal reactor made by Thomas Swan. The growth temperature and pressure were respectively 918 K (645 °C) and 350 Torr. The sources were trimethylindium, trimethylgallium, tertiarybutylarsine and tertiarybutylphosphine.

The active region of the laser structures consists of six 6.5 nm wide 1% compressive strain QWs (figure 2). The barriers are made of lattice matched 1.25 μm wavelength InGaAsP (1.25 Q). The first and last barriers are 17 nm thick and between the QWs the barriers are 5.5 nm thick. On each side of the QW stack the SCL are 100 nm thick and made of 1.15 μm wavelength InGaAsP (1.15 Q). The photoluminescence wavelength of structures W and W/O is 1.5 μm. On the p-side of the structure, the first 130 nm of InP cladding layer next to the SCL were not intentionally doped (nid) to prevent back diffusion of Zn into the SCL. The thickness of the $In_{0.81}Ga_{0.19}P$ layer is 6 nm in structure W.

Ridge waveguide broad area lasers with 57 μm wide stripes were processed. The as-cleaved lasers were characterized under pulsed conditions (0.05% duty cycle, 500 ns pulses) for temperatures ranging from 290 K (17 °C) to 390 K (117 °C).

3. Experimental results

At first order, assuming the internal absorption loss α_i and internal quantum efficiency η_i to be constant above threshold

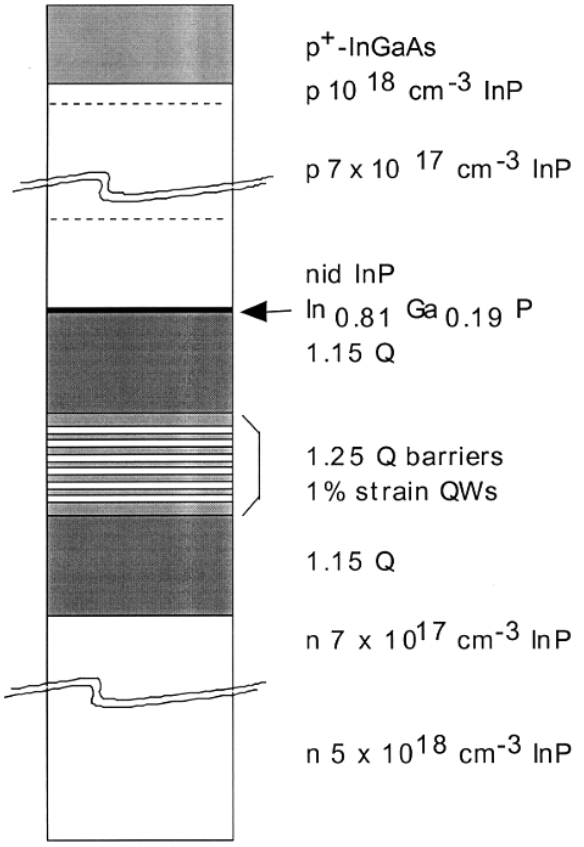

Figure 2. Structure of laser W with an $In_{0.81}Ga_{0.19}P$ electron stopper layer.

and independent on the length of the cavity, the differential quantum efficiency η_d can be related to α_i and η_i by:

$$\frac{1}{\eta_d} = \frac{\langle \alpha_i \rangle}{\eta_i \ln(1/R)} L + \frac{1}{\eta_i} \tag{1}$$

where R is the mean reflection coefficient of the laser facets and L is the cavity length. Cavity lengths between 250 μm and 1 mm were utilized to measure α_i and η_i using equation (1). Five to ten lasers of each cavity length were studied experimentally. Within a set of devices, the measured differential quantum efficiencies and threshold currents were within $\pm 4\%$. For each set of lasers the best, in terms of threshold current and differential quantum efficiency, was used for the temperature study.

Table 1 compares the properties of structures W and W/O at 293 K (20 °C). In addition to α_i and η_i, the threshold current densities per QW for 700 μm long cavities J_{th} and for infinite cavity length $J_{th\infty}$, the transparency current density per QW J_{tr} and the modal gain at threshold per QW were also measured. The values reported here are characteristic of state of the art lasers. In particular, the threshold current density for infinite cavity length is among the lowest reported. For ridge waveguide broad area lasers it is an important quality criterion because it only depends on the intrinsic quality of the active region. T_0 was calculated for 700 μm long cavity lasers for temperatures ranging between 293 K (20 °C) and 333 K (60 °C). Whereas an improvement of the internal quantum efficiency η_i and of the T_0 of structure W could be expected,

Table 1. Comparison of results for laser structures W/O and W at 293 K (20 °C). η_i is the internal quantum efficiency, α_i the internal absorption loss, J_{th} the threshold current density per QW for 700 μm long cavities, $J_{th\infty}$ the threshold current density per QW for infinite cavity length, J_{tr} the transparency current density per QW and g_{th} the modal gain at threshold per QW. T_0, the characteristic temperature of the threshold current, was calculated for temperatures between 293 K (20 °C) and 333 K (60 °C).

	Structure W/O	Structure W
η_i	0.69	0.67
α_i (cm^{-1})	9.7	11.2
J_{th} (A cm^{-2})	73	83
$J_{th\infty}$ (A cm^{-2})	56	61
J_{tr} (A cm^{-2})	45	48
g_{th} (cm^{-1})	8.3	8.2
T_0 (K)	61	59

Table 2. Critical and characteristic temperatures of structure W and W/O for 250 μm long laser cavities.

Structure W/O $T_c \approx 370$ K		Structure W $T_c \approx 370$ K	
$T < T_c$	$T > T_c$	$T < T_c$	$T > T_c$
$T_0 = 52$ K	$T_0 = 24$ K	$T_0 = 48$ K	$T_0 = 20$ K
$T_{\eta d} = 113$ K	$T_{\eta d} = 15$ K	$T_{\eta d} = 164$ K	$T_{\eta d} = 16$ K

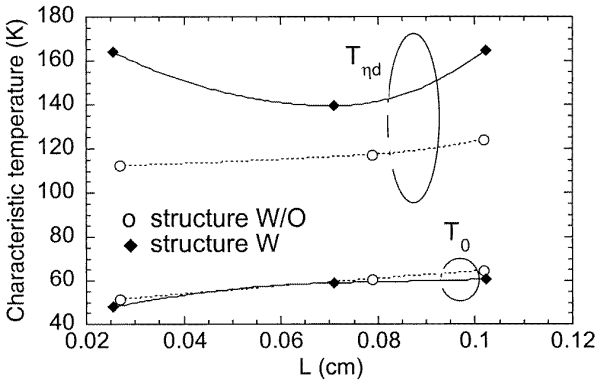

Figure 3. Experimental dependence of the characteristic temperatures T_0 and $T_{\eta d}$ on the cavity length of the laser structures W and W/O for $T < T_c$.

they are comparable to those of structures W/O. All the other properties also show almost identical results. The largest differences are with the internal absorption losses and the threshold current densities that are respectively 15 and 14% higher in W than in W/O. It seems that the InGaP layer results in higher SCL carrier densities which causes more absorption.

The way the differential quantum efficiency changes with respect to the temperature was also estimated using a characteristic temperature $T_{\eta d}$. The relation used for the fit is

$$\eta_d = \eta_{d0} \exp(-T/T_{\eta d}). \tag{2}$$

There is a critical temperature T_c that separates two regions where I_{th} and η_d have different temperature dependencies [14].

Table 2 shows the values of the critical temperatures T_c and the characteristic temperatures T_0 and $T_{\eta d}$ above and below T_c for both structures for 250 μm long lasers. The only

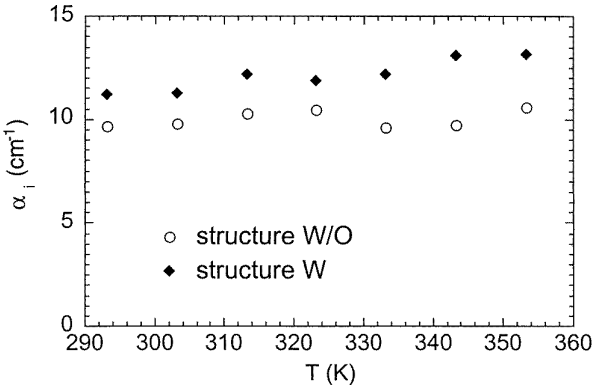

Figure 4. Experimental internal loss of laser structures W and W/O as a function of temperature.

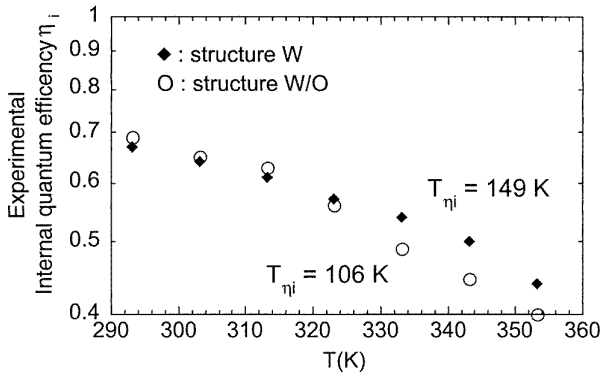

Figure 5. Experimental internal quantum efficiency of laser structure W and W/O as a function of temperature.

clear difference between the two structures is with $T_{\eta d}$ below T_c. It increases from 113 K to 164 K when adding the $In_{0.81}Ga_{0.19}P$ electron barrier layer whereas above T_c the $T_{\eta d}$ values are about the same. The improvement of $T_{\eta d}$ is observed whatever the laser length (figure 3). In contrast, the T_0 values (below T_c) of structures W and W/O are close to each other for all the lengths measured.

Figure 4 shows the internal absorption loss for laser structures W and W/O as a function of the temperature below T_c. The variation of α_i for both structures is very similar. It means that the higher value of $T_{\eta d}$ for structure W is essentially due to the higher value of the characteristic temperature of the internal quantum efficiency $T_{\eta i}$ (see figure 5). $T_{\eta i}$ is defined in the same way as $T_{\eta d}$ in equation (2).

For temperatures above T_c, the characteristic temperatures of structures W/O and W degrade strongly and are again the same. The two structures behave again identically. This catastrophic degradation of InGaAsP long-wavelength laser performance at high temperature has been attributed to a pile-up of carriers, in particular holes, in the SCL [14]. At high temperature, due to the small conduction band offset of this system (only 40% of the band gap energy difference is in the conduction band offset) electrons leak out of the QWs into the SCLs. This unbalances the charge distribution between the QWs and the SCLs and creates an electric field that traps holes in the SCLs. The charge accumulation in the SCL increases significantly the internal absorption loss and

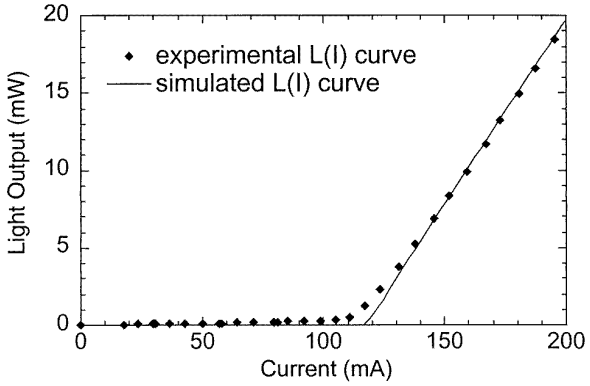

Figure 6. Comparison of measured and simulated light curve at room temperature. The width of the stripe is 57 μm and the length of the cavity is 270 μm.

recombination in the SCL that dominate and determine the temperature behaviour at high temperature.

Our observations are consistent with that explanation. First, the critical temperature is the same for structures W and W/O because it only depends on the conduction band offset between the QWs and the barriers. Second, a strong increase of the internal absorption loss accompanies the catastrophic degradation of the laser performance. In structure W/O the internal absorption loss at 363 K (90 °C) is 17.4 cm^{-1}. It is a 64% increase compared to the absorption loss at 353 K (80 °C) whereas the absorption loss increases by only 10 to 15% in the 293 K to 353 K (20 to 80 °C) range. Third, above T_c, the $T_{\eta d}$ values of structures W and W/O are again comparable because the electron barrier layer of structure W is outside the SCL and has no effect to prevent the pile-up of carriers in the SCL.

4. Analysis

An advanced laser simulation software [13] is used to analyse the effect of loss mechanisms on the temperature sensitivity of our laser diodes. The software calculates the optical gain in strained quantum wells based on the 4×4 $\boldsymbol{kp}$ method including valence band mixing and carrier–carrier interaction. The computed photoluminescence spectrum as well as the gain peak wavelength agrees well with our measured data. Carrier densities in the QWs are calculated assuming thermal equilibrium between carriers inside and outside the QWs. MQW intervalence-band absorption (IVBA) of $\alpha_{IVBA} = k_p p$ is considered which depends on the local density of holes (p) within the quantum wells ($k_p = 35 \times 10^{-18}$ cm^2 [15]). With higher temperature, IVBA is expected to exhibit an Arrhenius type increase with an activation energy of 13 meV [16]. Other important simulation parameters are the coefficients of Shockley–Read–Hall (SRH) recombination ($A = 10^{-8}$ s^{-1}), spontaneous emission ($B = 10^{-10}$ cm^{-3} s^{-1}) and Auger recombination ($C = 8 \times 10^{-29}$ cm^{-6} s^{-1}). The parameter C is considered temperature dependent with an Arrhenius type activation energy of 40 meV [17]. C was slightly adjusted to fit the measured threshold current of 118 mA for structure W/O at room temperature. Excellent agreement with the light

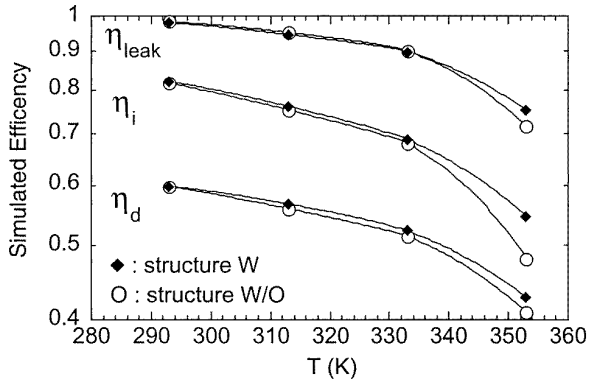

Figure 7. Calculated external differential quantum efficiency η_d, internal quantum efficiency η_i and leakage related differential efficiency η_{leak} of structures W/O and W as a function of temperature.

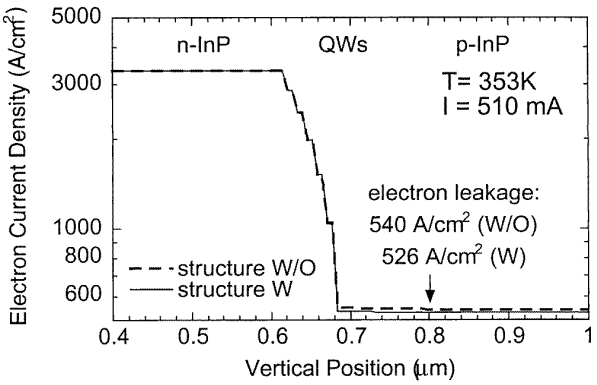

Figure 8. Calculated electron current density of structures W/O and W as a function of the vertical position in the laser structures.

versus current measurement is obtained at room temperature for structure W/O (figure 6).

Calculations for structures W and W/O give the same threshold current and the same slope efficiency at room temperature. The magnitude of the SCL absorption is not changed automatically by the software with changing SCL carrier density. A constant value of $\alpha_{SCL} = 13.7\ \mathrm{cm}^{-1}$ is assumed in all calculations. Since all other loss mechanisms are included, deviation of the calculated threshold current of structure W from the measured threshold current can be related to changes of α_{SCL} (figure 4). The reason is that due to its conduction band offset with InP the InGaP layer introduces a small additional resistance. This is evidenced by a discontinuity of the electron quasi-Fermi level in the InGaP layer in the calculated energy band diagram of the device in figure 1. The additional resistance requires the voltage across the structure to be slightly higher to obtain the same current. Compared to structure W/O this raises the Fermi level in the SCL and thus increases the carrier density and the absorption loss in the SCL. Some other additional effects may also contribute to the observed difference between the absorption loss of structures W and W/O.

The current calculation is based on a drift-diffusion model including thermionic emission at hetero-barriers. Thermionic emission of electrons from the SCL can be identified as minority carrier current in the p-InP cladding

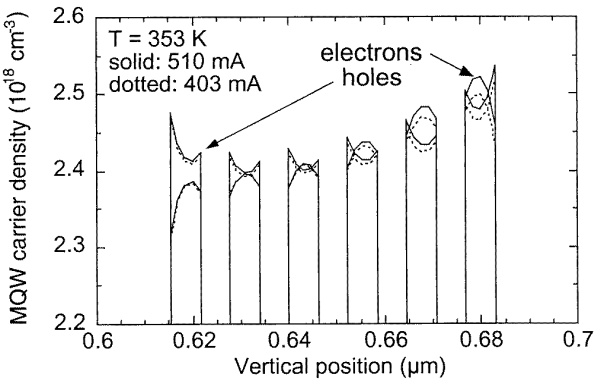

Figure 9. Calculated electron and hole density in the QWs in structure W for two biases above threshold.

layer. The increment of this electron leakage current divided by the increment in total current above threshold leads to a leakage related differential efficiency η_{leak} that is found to be 98% in both devices at $T = 293$ K (20 °C). Thus, leakage losses are quite small in our case and the InGaP stopper layer cannot have much effect at room temperature. This picture changes at higher temperature. Figure 7 plots the calculated reduction of slope efficiency η_d, internal efficiency η_i, and leakage related efficiency η_{leak} for both devices. Up to $T = 333$ K (60 °C), η_{leak} remains above 90% and the effect of the InGaP layer is negligible. But at $T = 353$ K (80 °C), η_{leak} is strongly reduced, indicating escalating electron leakage due to the spreading of the Fermi distribution of electrons towards higher energies. Under these conditions, the InGaP layer starts to be beneficial in reducing electron losses. Figure 7 gives differential changes above the threshold. The *absolute* leakage current reduction at 353 K is visible in a plot of the electron current density of both structures (figure 8). Electrons are injected into the MQW from the n-InP on the left-hand side and mostly recombine within the MQW, but a small electron current remains on the right-hand side in figure 8, indicating electron leakage into the p-InP cladding. With stopper layer, this leakage current is slightly smaller (solid line). For a vertical position of 0.8 μm in figure 8 it reduces from 540 to 526 A cm^{-2}.

The slope efficiency η_d in figure 7 also decreases with higher temperature but not as strongly as measured due to the constant absorption coefficient α_{SCL} in our calculation. In reality, α_{SCL} increases with higher temperature due to a higher SCL carrier density. In agreement with the experimental technique, the internal efficiency η_i in figure 7 is calculated from simulations at different laser lengths using equation (1). The computed values of $\eta_i(T)$ are within the standard deviation of the experiment (the plot $\eta_d^{-1}(L)$ results in different η_i if unreasonable η_d data are excluded). However, the $\eta_i(T)$ calculation clearly shows the measured impact of the InGaP layer at higher temperature (80 °C) due to reduced electron leakage.

A striking feature of figure 7 is the difference between η_i and η_{leak}. According to standard textbooks [18], both numbers should be identical in ridge waveguide broad area lasers with negligible spreading current loss as long as all recombination losses are clamped above threshold. Thus, the difference indicates that our recombination losses

increase above threshold. The calculated increment in SCL recombination per mA injection current is orders of magnitude too small to explain the efficiency difference. The answer must be related to quantum well recombination losses. Figure 9 shows the calculated density of electrons and holes within the MQW at two bias points above threshold. The quantum well closest to the p-doped side exhibits the highest carrier density. This is produced by the large effective mass of holes and the large valence band offset between the QWs and the barriers. It makes hole transport across the QW difficult. By Coulomb attraction the electron concentration also increases in the QWs close to the p-doped side. The non-uniformity of the carrier distribution becomes stronger as the injection current rises. This effect is well known for laser diodes that employ a larger number of quantum wells [19]. Thus, recombination losses within the QWs increase as well and cause the observed difference between internal efficiency η_i and leakage related efficiency η_{leak}. Auger recombination, whose recombination rate is proportional to the cube of the carrier density, is the predominant recombination loss. In fact, recombination losses contribute more to the low internal efficiency of our lasers than leakage losses.

5. Conclusion

We proposed a simple way to increase the electron confinement in the SCL of long-wavelength lasers by introducing an InGaP electron barrier layer on the p-side of the SCL. The comparison of the behaviour of laser structures with and without that confinement layer made it possible to demonstrate that current leakage over the SCL–p-cladding interface is not the dominant carrier loss mechanism at room temperature. The comparison of our experimental results with simulations shows that the internal quantum efficiency is reduced by the non-homogeneity of the carrier distribution among the QWs. This non-homogeneity increases with increasing current above threshold and it leads to increasing recombination losses.

The effect of the InGaP stopper layer is to improve the internal quantum efficiency of the laser above 333 K (60 °C) but below the critical temperature T_c of 370 K (97 °C). It also slightly increases the carrier density in the SCL. That higher carrier density increases the absorption loss and the threshold current compared to a structure without an electron stopper layer. Due to the small conduction band offset in the InGaAsP system the band bending in the SCL above T_c produces a carrier pile-up that degrades dramatically the performances of the laser. In that regime the increase of the electron confinement in the SCL does not have any effect to improve the behaviour of the laser.

Acknowledgment

This work was supported by the Center for Multidisciplinary Optical Switching Technology (MOST), a DARPA-sponsored MURI (Multidisciplinary Research Initiative).

References

[1] O'Reilly E P, Jones G, Silver M and Adams A R 1996 *Phys. Status Solidi* B **198** 363–73
[2] Andrekson P A, Kazarinov R F, Olson N A, Tanbun-Ek T and Logan R A 1994 *IEEE J. Quantum Electron.* **30** 219–21
[3] Belenky G L, Reynolds C L, Kazarinov R F, Swaminathan V, Luryi S L and Lopata J 1996 *IEEE J. Quantum Electron.* **32** 1450–5
[4] Kazarinov R F and Belenky G L 1995 *IEEE J. Quantum Electron.* **31** 423–6
[5] Ohshima T, Moriguchi H, Shigemasa R, Gotoh S, Tsunotani M and Kimura T 1998 *Proc. 10th Int. Conf. on Indium Phosphide and Related Materials (Tsukuba, 1998)* (New York: IEEE) pp 761–4
[6] Borchert B, Gessner R and Stegmüller B 1994 *Japan. J. Appl. Phys.* **33** 1034–9
[7] Murai H, Matsui Y, Ogawa Y and Kunii T 1995 *Electron. Lett.* **31** 2105–7
[8] Takemasa K, Munakata T, Kabayashi M, Wada H and Kamijoh T 1998 *Proc. 10th Int. Conf. on Indium Phosphide and Related Materials (Tsukuba, 1998)* (New York: IEEE) pp 835–8
[9] Ubukata A, Dong J and Matsumoto K 1998 *Proc. 10th Int. Conf. on Indium Phosphide and Related Materials (Tsukuba, 1998)* (New York: IEEE) pp 721–4
[10] Loh T, Miyamoto T, Koyama F and Iga K 1995 *Japan. J. Appl. Phys.* **34** 1504–5
[11] Bensaada A, Graham J T, Brebner J L, Chennouf A, Cochrane R W, Leonelli R and Masut R A 1993 *Appl. Phys. Lett.* **64** 273–5
[12] Van de Walle C G and Martin R M 1986 *Phys. Rev.* B **34** 5621–34
[13] PICS3D by Crosslight Software Inc. (details at www.crosslight.ca)
[14] Seki S, Oohashi H, Hirono T and Yokoyama K 1996 *IEEE J. Quantum Electron.* **32** 1478–85
[15] Joindot I and Beylat J L 1993 *Electron. Lett.* **29** 604–6
[16] Regelmann D 1998 unpublished calculation
[17] Silver M 1997 Personal communication
[18] Coldren L A and Corzine S W 1995 *Diode Lasers and Photonic Integrated Circuits* (New York: Wiley)
[19] Grupen M and Hess K 1998 *IEEE J. Quantum Electron.* **34** 120–40